University of Glasgow | Experimental Particle Physics

GLAS-PPE/2008-21
25th November 2008

Department of Physics and Astronomy
Experimental Particle Physics Group
Kelvin Building, University of Glasgow,
Glasgow, G12 8QQ, Scotland
Telephone: +44 (0)141 330 2000 Fax: +44 (0)141 330 5881

JETS AND MEASUREMENTS OF α_s

P. J. Bussey

For the H1 and ZEUS Collaborations. [1)]

Abstract

A survey is presented of recent measurements in jet physics, and improved determinations of the QCD coupling constant α_s that these have made possible.

NEW TRENDS IN HERA PHYSICS
RINGBERG CASTLE, GERMANY, OCTOBER 2008

[1)] Royal Society of Edinburgh/ Scottish Executive Support Research Fellow

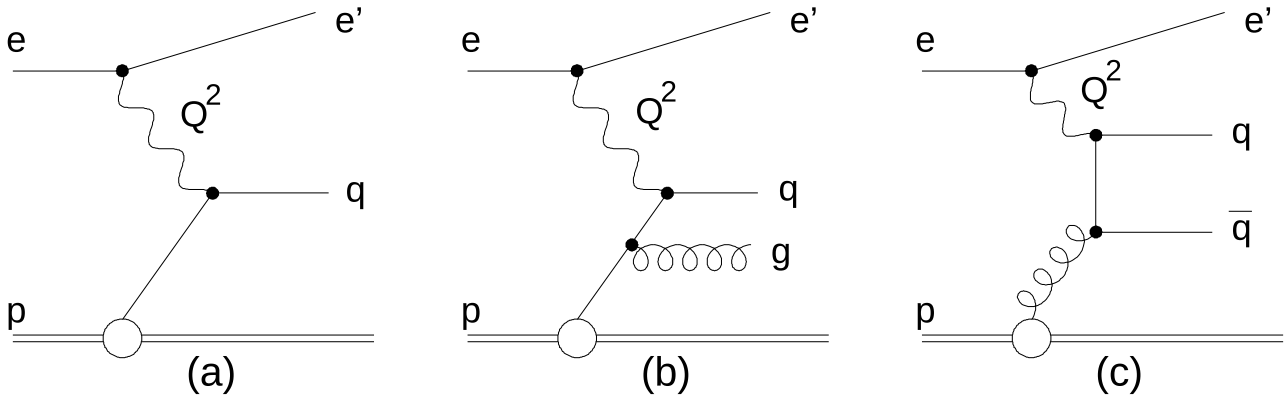

Figure 1: Examples of hard QCD processes at order zero and unity in α_s.

1 INTRODUCTION

Following the first realisation that hadronic particles consist of charged fermions known as quarks, held together by bosonic particles known as gluons, it was learnt that the quarks and gluons ("partons") can never be observed on their own. Any attempt to isolate a quark, for example by knocking it violently out of a hadron in an energetic collision process, does not result in an observable quark (or gluon). Instead, a shower of elementary particles is seen, referred to as a jet, containing the energy of the original quark or gluon. The gluons couple to the quarks by a running coupling constant α_s.

In this account, we first make some brief notes regarding QCD processes. There follows a survey of recent experimental results regarding jet measurements and what has been learned from them. In particular, we then examine some recent measurements of α_s and attempt to make some comparisons.

2 STATUS OF CALCULATIONS

The most basic diagram in deep inelastic scattering (DIS) consists of an incoming lepton exchanging a virtual boson (photon or electroweak) with a quark in an incoming hadron (Fig. 1(a)). The quark is ejected to give rise to an observable jet. The coupling of the virtual boson to the lepton and the parton is electromagnetic or electroweak, and α_s is not directly involved.

Higher order processes involve the radiation of gluons at various points. The outgoing quark may radiate a gluon, or an incoming quark may do so, in which case the exchanged boson may interact with it by means of a quark pair, a process known as boson gluon fusion. These processes are illustrated in Figure 1(b), (c) and are of order unity in α_s. Processes of higher order in α_s have also been studied and will be discussed below.

At present [1], all the relevant QCD processes at lowest order (LO) in α_s have been calculated, and also all the next-to-leading order (NLO) processes involving two partons entering and two leaving. Most of the NLO processes involving the radiation of a third particle have also been calculated, but little has been done at higher order. The NLO calculations, as we shall see, are in good agreement with the relevant measurements at HERA. However theory errors are beginning to become dominant in the α_s determinations, raising the issue of how to obtain increased theoretical accuracy.

3 EXPERIMENTAL METHODS

The experimental methodology for measuring jet cross sections is by now, in principle, well established. It is taken that the jet corresponding to a quark or gluon radiated in a hard process, namely at high transverse momentum p_T, will comprise particles that are in a definable sense close together. Two main approaches are now adopted: to define the closeness in terms of a cone angle in η, ϕ space, where η is pseudorapidity and ϕ is angle, or to use a clustering method. With cones, a cone radius is specified and particles are accepted if they are all found in one cone. Subtleties arise in connection with the basic cone search, and in cases where jets overlap. With clustering techniques a parameter is defined involving the transverse energies of two objects and their angular separation in η, ϕ, and clustering is performed iteratively between objects (including already clustered objects) whose clustering parameter is less than a given value.

The complicating issues here arise in connection with the comparison with theory. In theoretical calculations at a given order we will just have distributions of partons, and it will be desired to apply the same jet algorithm to these to determine the jet properties at the parton level. If only one parton were to be involved there is no problem. However this will not be the case owing to the radiation of extra partons, and these processes tend to have infra-red and collinear divergences; the jet algorithm must not be disturbed by these if we are to have a definable correspondence between the parton jets and the hadronic jets, with just a hadronisation correction to be evaluated and applied.

The effects in question tend to be small in magnitude and were ignored for many years in the context of cone jets, but this is no longer acceptable if we are dealing with high order processes or precision measurements. Clustering approaches are much less problematic, and have become standard practice at HERA; however with many-jet events the well-defined radius of a cone can give advantages. The mid-point algorithm, which performs a second iteration in its cone search, using seeds midway between the jets already found, is helpful but not perfect. Recent developments here include SISCone (Seedless Infrared Safe cone) and the so-called "anti-kT" algorithm. These approaches should serve well at the LHC. For a more detailed account of these issues, the reader should consult the account here by C. Soyez [2].

The experimental approach, then, is to use a jet finder that will give an adequate relationship between experiment and theory, and check that the basic kinematic distributions of jet quantities agree with the QCD calculation of choice. It will also be necessary to use a trusted set of parton densities (PDFs) in the proton. Discrepancies may indicate the need for more accurate PDFs. If all is well, the data may be used to extract a value of α_s, provided that the process studied involves diagrams that are of at least order unity in α_s. A high-order process would give greater sensitivity but may well not have been calculated. These tasks, of course, may not be completely separable.

4 TEVATRON RESULTS

The highest jet energies at present are achieved at the Tevatron operating $p\bar{p}$ collisions at a centre of mass energy of 1.96 TeV. Both CDF and D0 have made extensive studies in the field of jets and their properties, and we show here some of their recent results [3, 4]. Figure 2 shows inclusive jet distributions as function of transverse energy for different rapidity ranges. Comparison is made with an NLO QCD calculation (NLOjet) and excellent agreement is observed, both in the shape of the distributions and in the absolute magnitude, in all ranges. The agreement in magnitude amounts largely to a confirmation of the CTEQ PDFs used, while the agreement in E_T shape points to the accuracy of the QCD calculations.

Both collaborations have also presented cross sections for prompt photon production, which tests different perspectives on QCD. CDF find good agreement with theory (JETPHOX) in their results, while D0 find some discrepancies with theory in their photon plus jet cross sections. The cause for these is not at present clear. CDF's dijet mass spectrum, measured up to 1400 GeV/c^2, again shows excellent agreement with NLO theory (NLOjet + CTEQ6.1M) with no signs of any additional structural features.

5 JETS IN PHOTOPRODUCTION

Figure 3 indicates the two main categories of process in hard photoproduction, at lowest order in α_s. In direct processes the photon couples directly to a high-p_T quark line, while in resolved processes, the photon interacts through a hadronic intermediate state to which it couples non-perturbatively; this state represents the "hadronic structure of the photon" and the hard scatter, describable perturbatively in QCD, takes place with one of the partons in this structure. The distinction between direct and resolved processes can be made also at higher order, but an arbitrary division must be made between them; only quark pairs with p_T above the so-called factorisation scale will be considered hard, while quarks at lower p_T values will be considered as constituting part of the hadronic structure of the photon.

The fraction x_γ of the photon energy that is taken by the jet system, for two or more jets, can be calculated from the kinematics of the jets. For a direct process it should ideally take the value of unity, but owing to hadronic effects and soft radiation its observed value is less than this. Direct-dominated and resolved-dominated processes can largely be separated experimentally by taking x_γ above and below a value of approximately 0.75.

ZEUS have published improved measurements of dijet production at HERA [5]. The shape of the E_T distribution is well described over more than three orders of magnitude (Fig. 4), while the predictions using two different hadronic models of the photon [6, 7] differ slightly for the resolved events; of course there is little difference between the photon models for the direct events, where the excellent agreement between theory and experiment confirms both the general theory and the choice of proton PDFs (CTEQ). The azimuthal angle between the jets, which at LO should be 180°, is sensitive to summed higher order effects including soft radiation. The hadronising Monte-Carlo HERWIG is found to model this distribution better than the standard parameters of PYTHIA, although the latter can in fact be tuned. (Fig. 5)

ZEUS have also studied multi-jet distributions with a view to checking the accuracy of higher order calculations, and also to ascertain whether a multi-parton description of the resolved photon-proton scatter should be employed. The distributions in E_T of the jets in three-jet and four-jet events, in various η intervals, are found to be satisfactory. There are some indications that multiple parton interactions (MPI) improve the description. However clearer indications come from the x_γ distributions (Fig. 6). For high masses of the jet system, direct processes dominate, but for low masses there is a substantial resolved component which is not well described without the MPI option to PYTHIA or HERWIG. Even here the agreement is not perfect, but at least the magnitude is well given. The effect is more pronounced in the four jet events, but is evident in the three-jet sample.

As a further study in photoproduction, ZEUS have used the angular correlations in three-jet events to compare the predictions of standard QCD with those from various alternative models [8]. The following parameters can be defined:

- θ_H = angle between plane of highest energy jet and beam, and plane of two lowest energy jets.
- α_{23} = angle between two lowest energy jets.
- β_{KSW} = Körner-Schierholz-Willrodt angle (based on cross products of jet vectors).
- $\eta^{\rm jet}_{\rm max}$ = maximum pseudorapidity of the three jets.

Distributions of these variables can then be compared with the predictions from different variant models. QCD makes use of the symmetry group SU(3); we can compare this with SU(N) with large N, $U(1)^3$ (no triple gluon coupling), and SO(3). The results, unsurprisingly but gratifyingly, favour standard QCD. Figure 7 illustrates some of the distributions. In each case, standard QCD fits the data well, while the other possibilities all fail in some regions of some of the plots.

6 EFFECT OF POLARISED BEAMS

Turning to deep inelastic scattering, we note that HERA II was able to deliver longitudinally polarised electron and positron beams. In the electroweak sector of the standard model, the charged-current (CC) jet cross sections are sensitive both to the polarisation and to the nature of the lepton beam. Since CC DIS converts the incoming lepton into a neutrino, the signature for this process is at least one p_T-imbalanced hard jet in the detector. The cross sections become measurable only at high values of the virtual boson mass squared Q^2. As in all the HERA measurements, a k_T cluster algorithm was used for jet identification.

Figure 8 illustrates the results obtained [9]. It is clear that the cross sections are much higher for positive polarisations than negative for a positron beam, and vice versa for an electron beam. Agreement with theory, using a ZEUS parameterisation of the proton PDFs, is very good, and was confirmed using the CTEQ6 and MRST2001 PDF sets. Comparable results are obtained for the cross sections as a function of E_T of the jets, and for the cross sections evaluated for zero beam polarisation. Here we are specifically testing electroweak theory in a new regime from the measurements at LEP.

7 BREIT FRAME MEASUREMENTS.

A good method for measuring $\alpha_{\rm s}$ in DIS is to determine the cross sections for different kinematic ranges as a function of Q^2 and make use of the DGLAP equations, which involve $\alpha_{\rm s}$, to describe the variation of the cross sections with Q^2 and the kinematic variables. A fit to the entire data set enables $\alpha_{\rm s}$ to be extracted.

Here, however, we concentrate on $\alpha_{\rm s}$ determinations which depend more explicitly on measuring jet cross sections. H1 have performed this task as follows. First, they take each event as viewed in the Breit frame and find jets using the k_T cluster method in this frame. In the Breit frame, the event axis is taken along the direction of the virtual photon, such that in a simple deep inelastic scatter (Fig. 1(a)) the quark is hit head-on and merely reverses its direction. Such scatters, although they are hard, have no transverse energy in the Breit frame. It follows that high-E_T jets in this frame result exclusively from higher order processes, namely those that involve non-zero powers of $\alpha_{\rm s}$. The sensitivity to $\alpha_{\rm s}$ is therefore enhanced by measuring jets in this way.

A laboratory rapidity cut is imposed in order to have well-defined acceptance for the jets, and a number of different differential cross sections are evaluated. Figure 9 shows normalised inclusive jet cross sections measured under these conditions, compared to a NLO calculation; similar distributions were obtained for two- and three-jet final states. The normalisation approach enables some of the experimental and theoretical uncertainties in $\alpha_{\rm s}$ to be reduced. This analysis was performed at high values of Q^2, which reduces some of the theoretical errors at the cost of poorer statistics. All the control plots gave good fits using the NLO theory. From a general fit to the data, α_s was evaluated as a function of Q^2.

In a second analysis, H1 used a lower range of Q^2, giving better statistics but, as we shall see, notably worse theoretical uncertainties. Events are selected in the range $5 < Q^2 < 100$ GeV^2 with the fractional virtual photon energy in the range $0.2 < y < 0.7$. Jets are selected, as before, in the Breit frame and must have $E_T > 5$ GeV. Detector effects are simulated and acceptances evaluated, as before, using standard Monte Carlos. General comparison is made with the NLOJET++ Monte Carlo predictions.

As is evident in Figure 10, there is a noticeable difference between the predictions for different choices of renormalisation scale. Both Q^2 and $(E_T^2 + Q^2)/4$ are plausible, but the former value provides a good fit to the data while the latter is barely acceptable. The difference between the final results obtained with these two choices must therefore be accounted as a theoretical uncertainty. Varying the factorisation scale likewise gives rise to a theoretical uncertainty on the results. The experimental systematics must likewise be included in the normal way, and variations in the chosen PDFs must also be taken.

For a series of Q^2 bands, double differential cross sections $d^2\sigma/dQ^2dE_T$ were evaluated for a set of jet E_T values. Fits varying α_s were carried out on these. The results are given in the next section.

8 RESULTS FOR α_s

Experimental values for α_s can be determined in various ways, and they are seen to fall with increasing values of the typical momentum scale, such as Q or an equivalent variable, demonstrating the running nature of this coupling constant. It is conventionally quoted at $Q^2 = M_Z^2$. At LEP, some accurate determinations have been made using the properties of event shapes. Dissertori et al [10] have used an NNLO QCD calcluation to fit ALEPH data and obtain

$$\alpha_{\mathrm{s(M_Z)}} = 0.1240 \pm 0.0008 \pm 0.0010 \pm 0.0011 \pm 0.0029$$

where the errors are, in order, statistical, systematic, hadronisation and theoretical. From an analysis of ALEPH and OPAL thrust data, and incorporating their own theoretical model, Becher and Schwartz [11] have obtained

$$\alpha_{\mathrm{s(M_Z)}} = 0.1172 \pm 0.0010 \pm 0.0008 \pm 0.0012 \pm 0.0012$$

Using an NNLO + NLLA ansatz, Bethke et al. [12] obtain from the JADE data

$$\alpha_{\mathrm{s(M_Z)}} = 0.1172 \pm 0.0006 \pm 0.0020 \pm 0.0035 \pm 0.0030.$$

These values have high numerical precision but have potential dependencies on the theoretical approach that is adopted.

From HERA we first examine the recent H1 high-Q^2 results, obtained from the data described above (Fig. 11), and representing a clear improvement on their publication of 2007 [13]. Sensitivity to α_s is increased by measuring events with differing numbers of jets. Having demonstrated that α_s runs as expected with Q^2, the group perform a combined fit and obtain the value

$$\alpha_{\mathrm{s(M_Z)}} = 0.1182 \pm 0.0008\ ^{+0.0041}_{-0.0031} \pm 0.0018.$$

The low-Q^2 results give a fitted value of

$$\alpha_{\mathrm{s(M_Z)}} = 0.1186 \pm 0.0014\ ^{+0.0132}_{-0.0101} \pm 0.0021$$

where the three uncertainties correspond to experiment(total), theory, and PDFs. These results (Fig. 12, top) have a very much larger theoretical uncertainty than the high-Q^2 set. However when the values obtained are plotted with the fitted values and certainties obtained from the high-Q^2 set extended down to lower Q^2, the agreement is perfect, indicating the consistency of the central values of the theoretical parameters applied over the whole range of Q^2. Given the smallness of the experimental compared to the theoretical uncertainties, the need for NNLO calculations is becoming increasingly evident.

ZEUS have evaluated α_s from some recent measurement of inclusive jets in photoproduction (Fig. 13), taking the MRST2001 and GRV-HO proton and photon structures as central values. They obtain

$$\alpha_{\mathrm{s(M_Z)}} = 0.1223 \pm 0.0001 \pm 0.0022 \pm 0.0030,$$

where the uncertainties are respectively statistical, systematic and theoretical. This is competitive with other values and in good agreement with them. In DIS, H1 and ZEUS have put together their results for HERA I inclusive jet data to produce a combined fit for α_s. Apart from the improved statistical accuracy, this approach allows for a correct account to be taken of systematic and theoretical effects which are common or correlated between the two experiments. From H1, 24 data points at different E_T are taken with $150 < Q^2 < 15000$ GeV^2, while ZEUS contributes six inclusive cross sections in the range $125 < Q^2 < 100000$ GeV^2. The QCD cross sections are calculated with NLOJET++. The factorisation scale is taken as Q, the renormalisation scale is taken as E_T of the jets, and the MRST2001 PDF sets are employed. A χ^2 matrix is defined and minimised using a Hessian method. The result is:

$$\alpha_{s(M_Z)} = 0.1198 \pm 0.0019(exp) \pm 0.0026(theory),$$

competitive with the LEP results.

Figure 14 illustrates results from the combined fit, showing the running of α_s with jet E_T, and also a collected set of $\alpha_s$values from a number of HERA analyses, again showing well the running of α_s with the relevant momentum scale. A collection of determinations of α_s is shown in Figure 15 in comparison with a recent world average value. It is clear that the different approaches are in general in good agreement. The tendency is also evident that in order to obtain small theoretical uncertainties, which in practice means using high momentum scales, a penalty of poorer statistics must be paid. This effect will become less evident if sufficient statistics become available to reduce the dominance of the statistical uncertainty, as is already the case in some analyses.

9 SUMMARY

In summary, the study of jet distributions at HERA, as at the Tevatron, has been a highly fruitful area to investigate a number of aspects of Quantum Chromo-Dynamics. The theory continues to pass all tests, and evaluations of the coupling constant α_s are being performed from a number of different perspectives. Accuracy is improving with the accumulation of larger data samples and further developments in the theoretical calculations that are available for the experimentalists to use. However there is an increasing need for more NNLO calculations. Nevertheless, this is impressive progress and should come to a fruition when the full HERA II analyses have been completed.

I should like to thank the organisers of the Ringberg 2008 workshop for all the efforts that they put in to ensure an outstandingly enjoyable and stimulating meeting.

References

[1] See G. Zanderighi, review talk at ICHEP 2008, hep-ph/0810.3524

[2] C. Soyez, these Proceedings.

[3] CDF Collaboration,T. Aaltonen et al, Phys. Rev. D 78, 052006 (2008)

[4] D0 Collaboration, V. Abazov et al, Phys. Rev. Lett. 101 062001 (2008)

[5] ZEUS Collaboration, S. Chekanov et al, Phys. Rev. D 76 (2007) 072011

[6] P. Aurenche, M. Fontannaz and J. Guillet, Eur. Phys. J C 34 (395) (2005)

[7] F. Cornet, P. Jankowski and M. Krawczyk, Phys. Rev. D 70, 093004 (2004)

[8] ZEUS Collaboration, S Chekanov et al., DESY-08-100, to be published in Eur. Phys. J D.

[9] ZEUS Collaboration, S Chekanov et al., Phys. Rev. D 78 (2008) 032004

[10] G. Dissertori et al., hep-ph/0712.0327v2

[11] T. Becher and M. Schwartz, hep-ph/08030342v2

[12] S. Bethke et al., hep-ex/0810.1389

[13] H1 Collab., A. Aktas et al., Phys. Lett. B653 (2007) 134

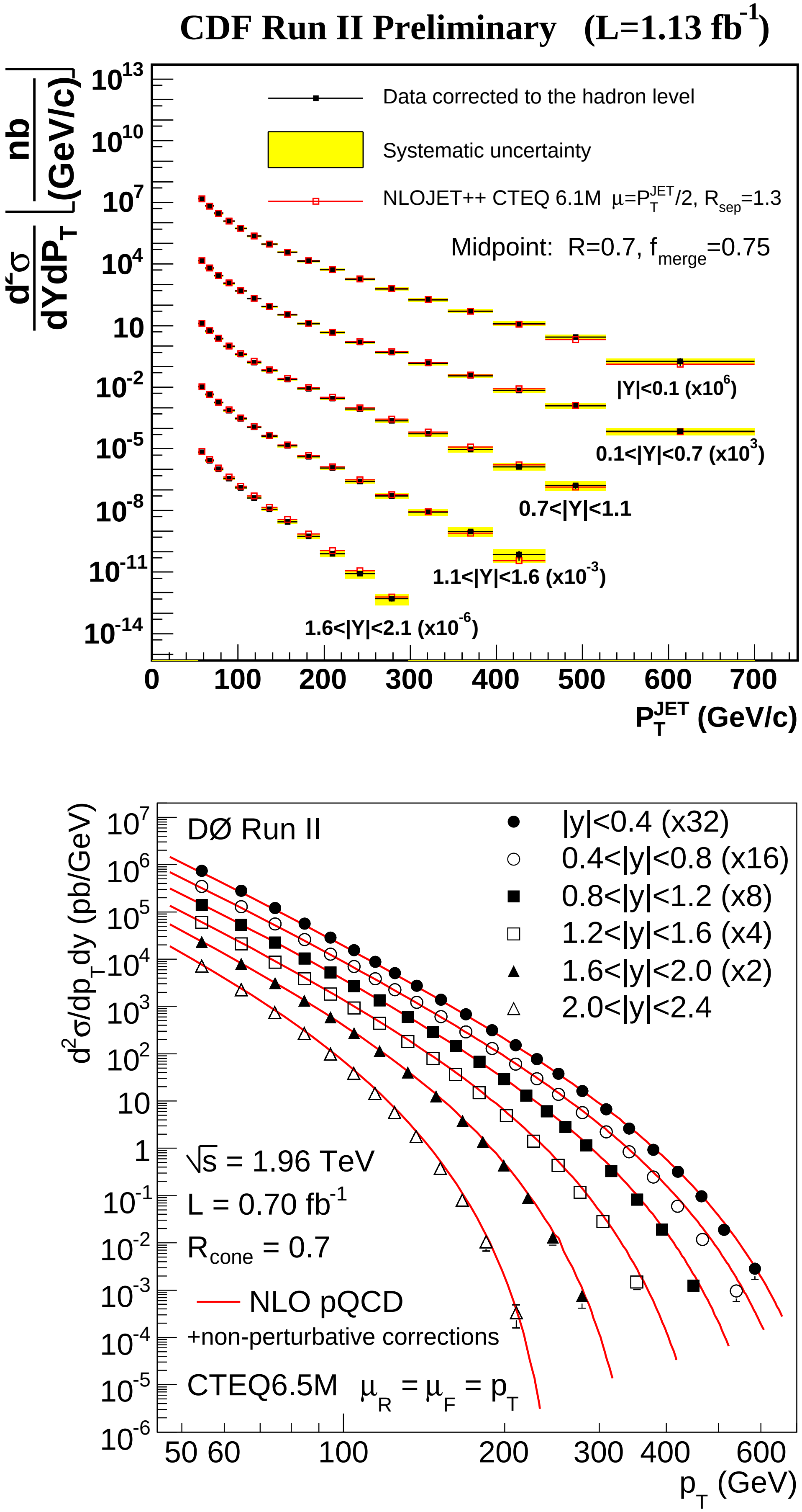

Figure 2: Jet distributions as a function of transverse energy from CDF and D0, using the mid-point algorithm with cone radius 0.7.

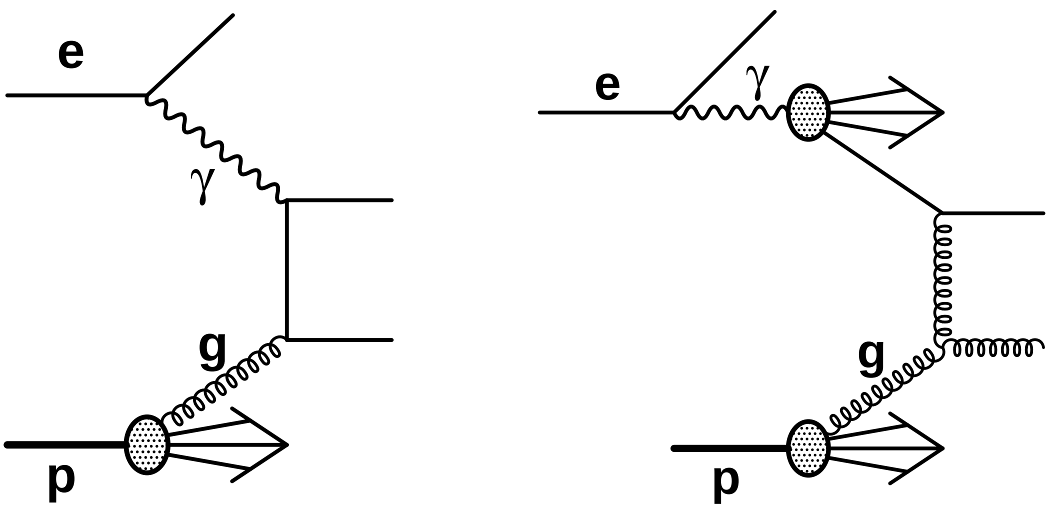

Figure 3: Direct and resolved processes at LO in photoproduction.

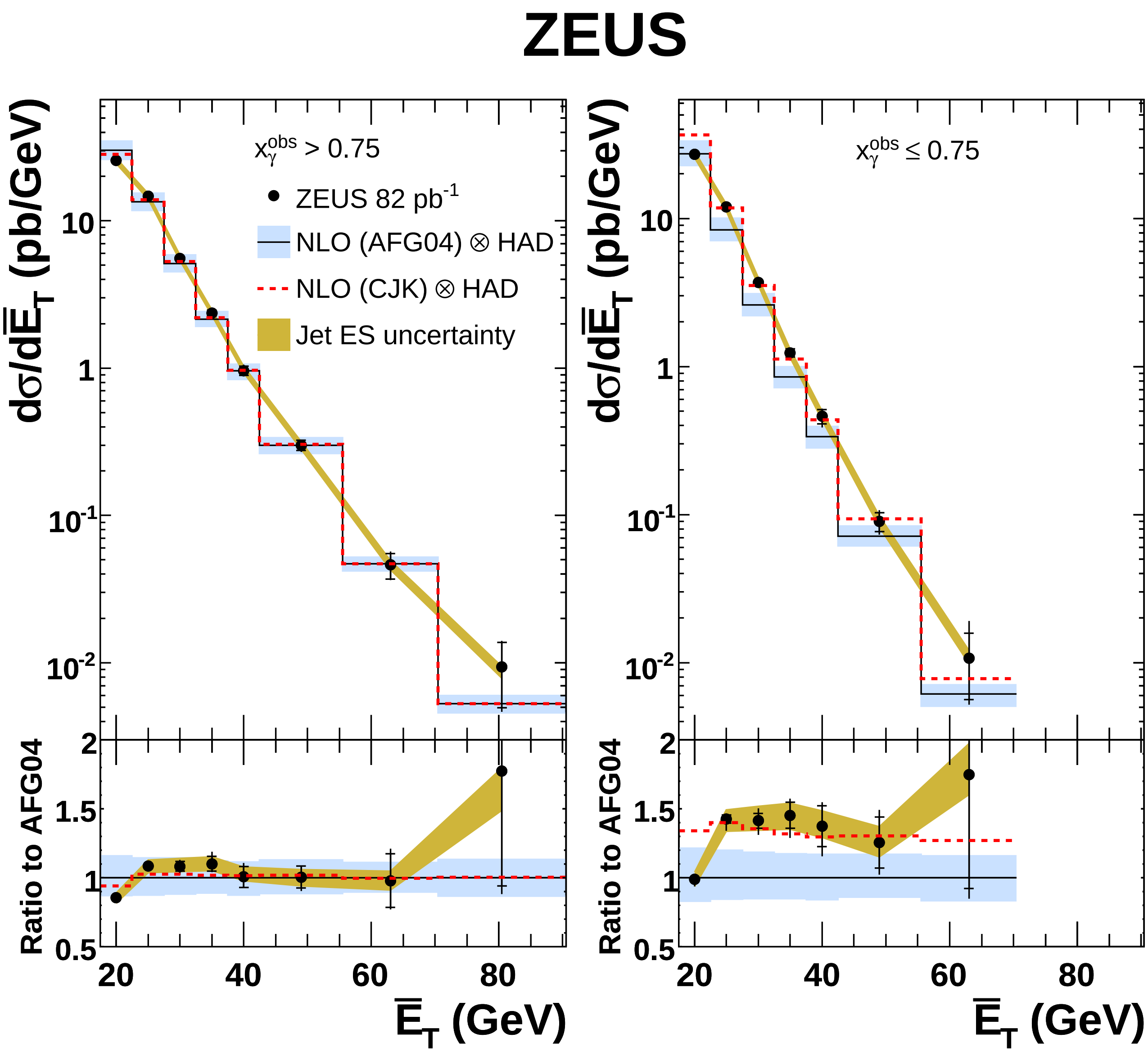

Figure 4: Distribution of the mean E_T of photoproduced dijets for direct-dominated and resolved-dominated event samples.

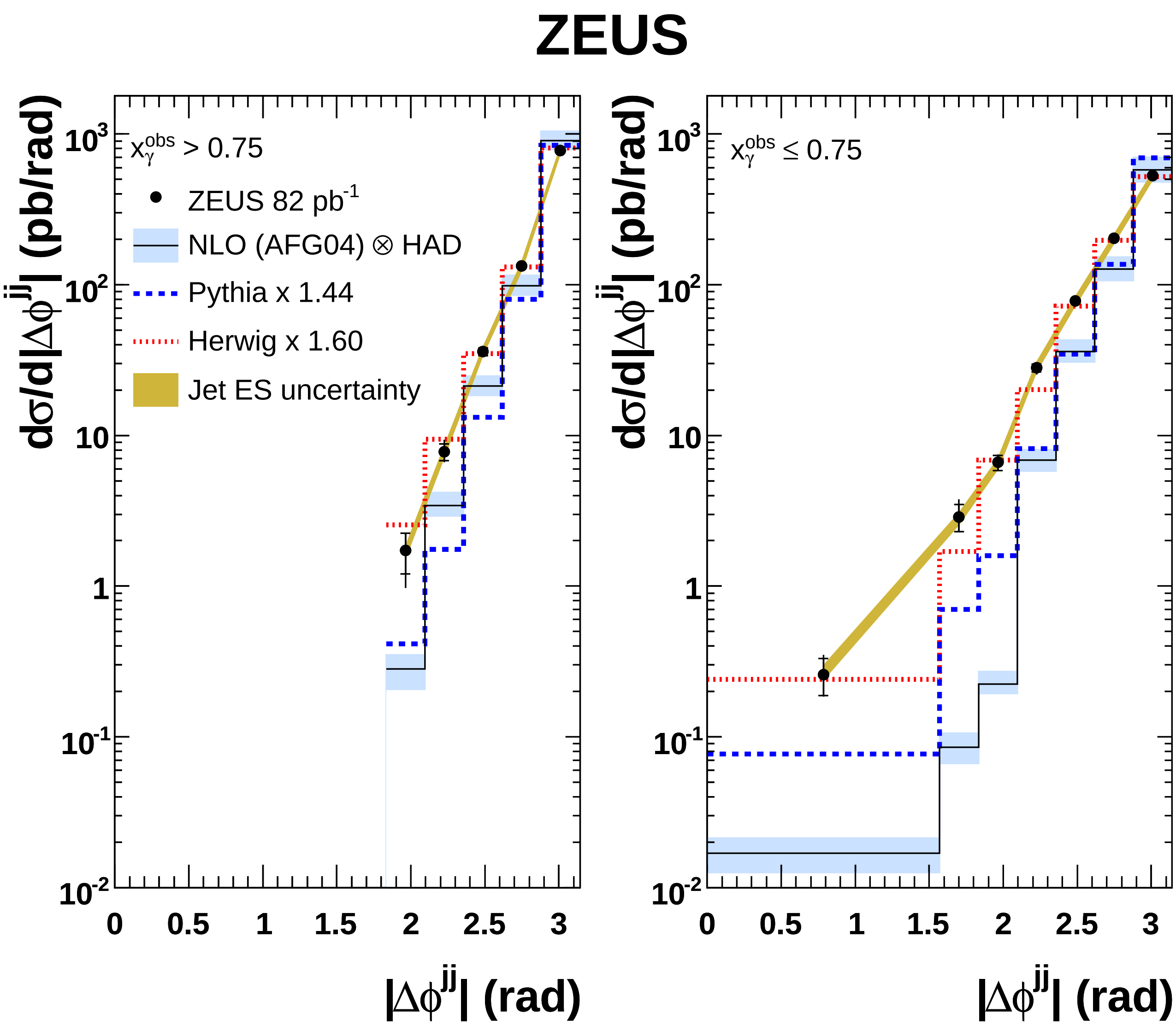

Figure 5: Azimuthal angle between the jets in the analysis of Figure 4, compared with different theoretical approaches, for direct-dominated and resolved-dominated event samples.

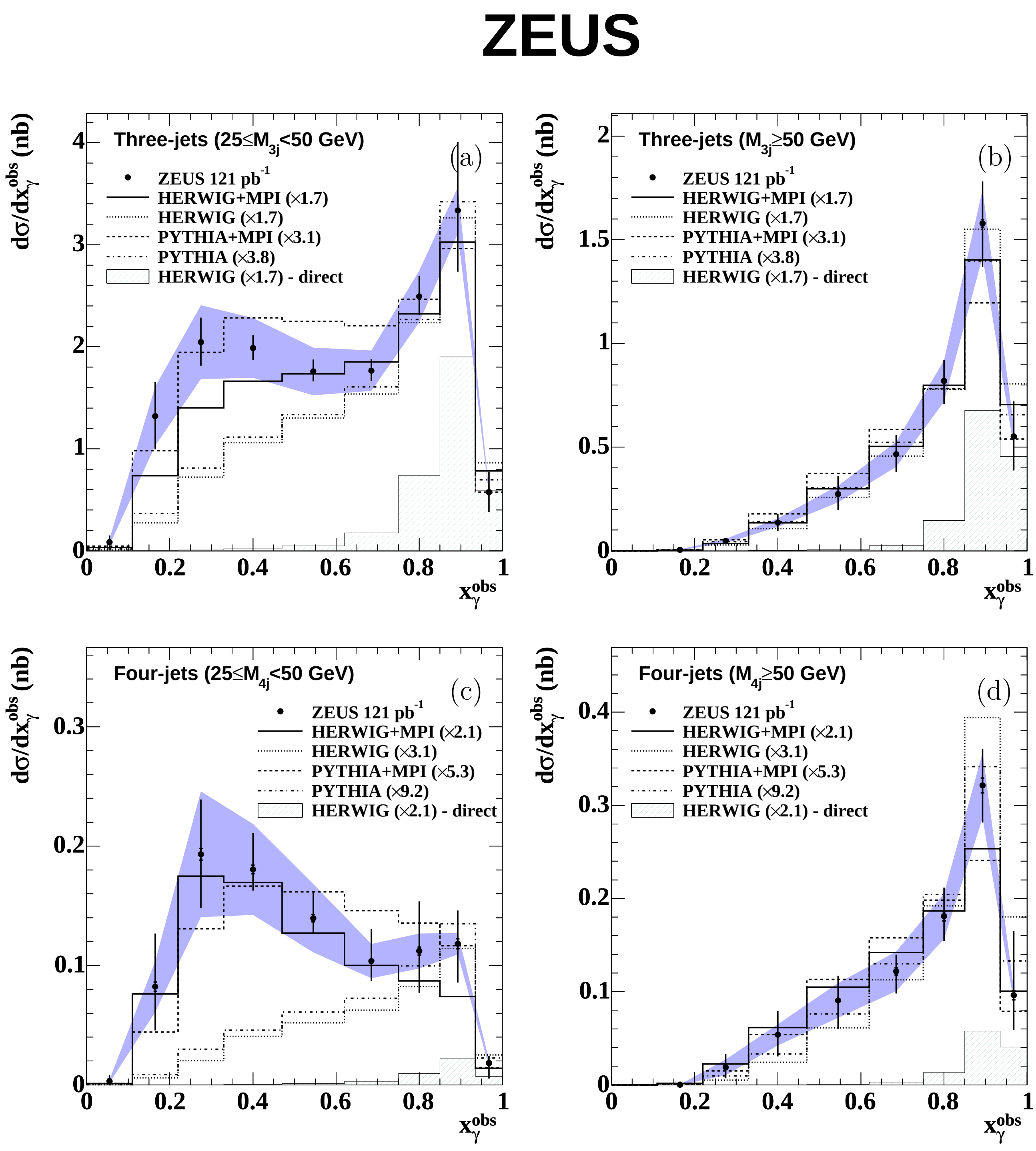

Figure 6: Distributions in the observed value of x_γ for three- and four-jet events for jet masses below and above 50 GeV.

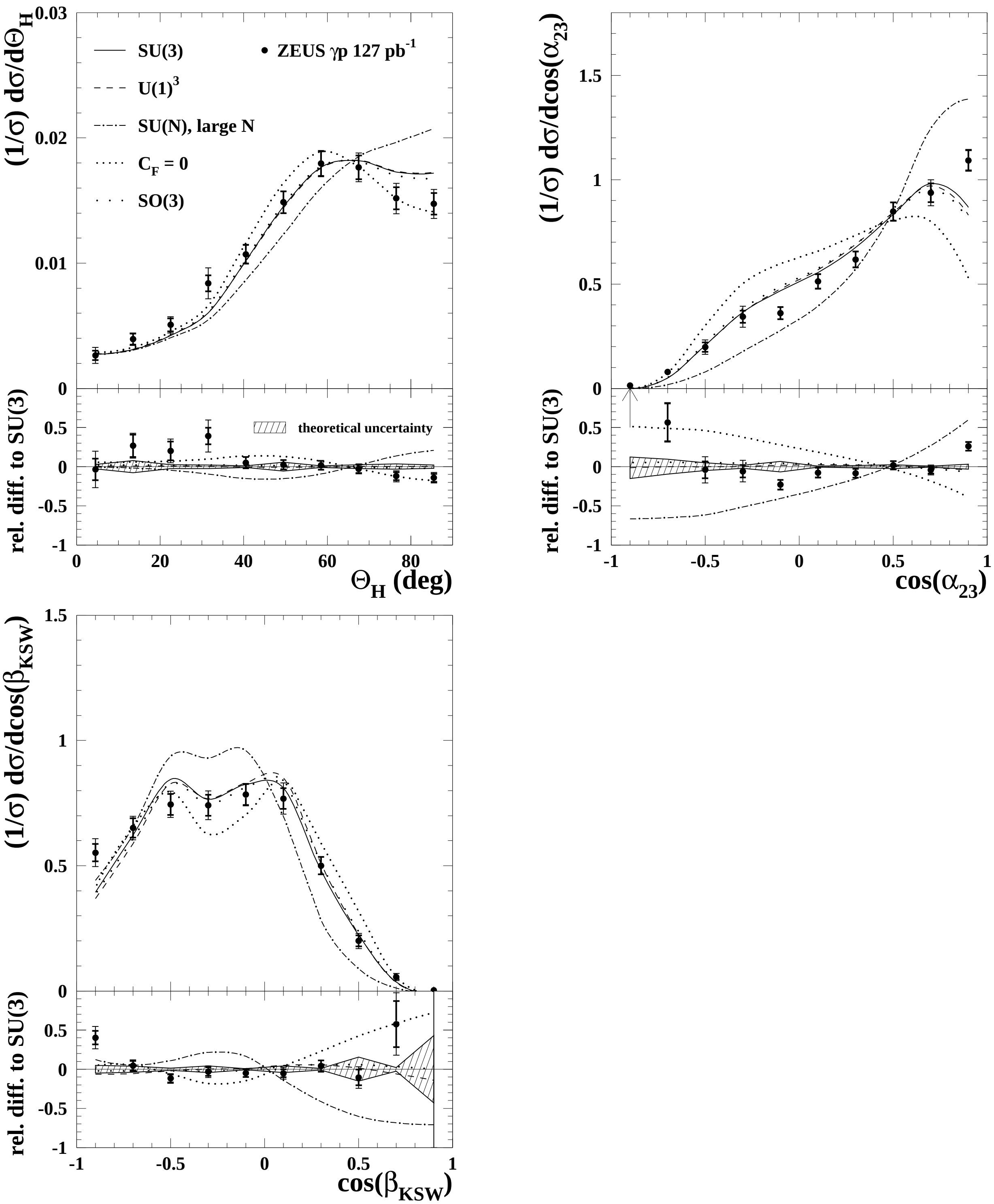

Figure 7: Distribution of angular parameters of the three-jet system with predictions from standard QCD (solid line) and several variant theories.

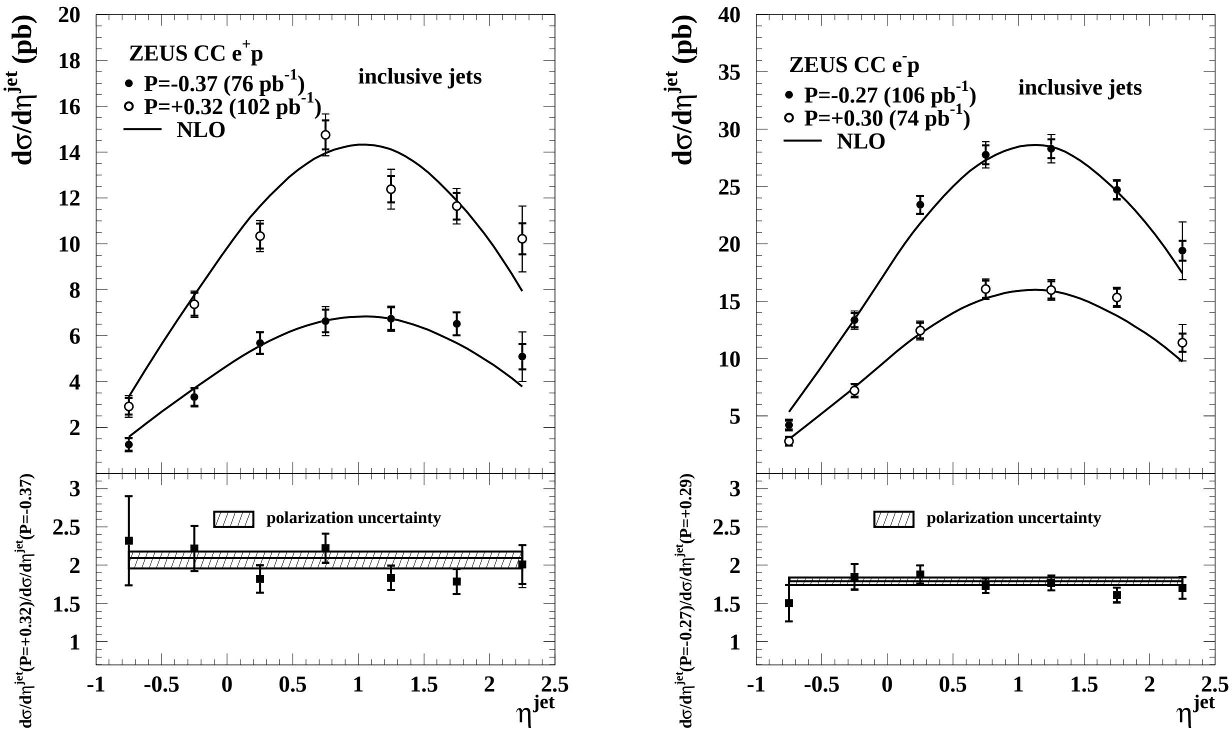

Figure 8: Cross section measured by ZEUS for inclusive jets in charged-current DIS for positron and electron beams, and opposite longitudinal electron/positron polarisations, compared to SM theory at NLO (MEPJET) as a function of jet pseudorapidity.

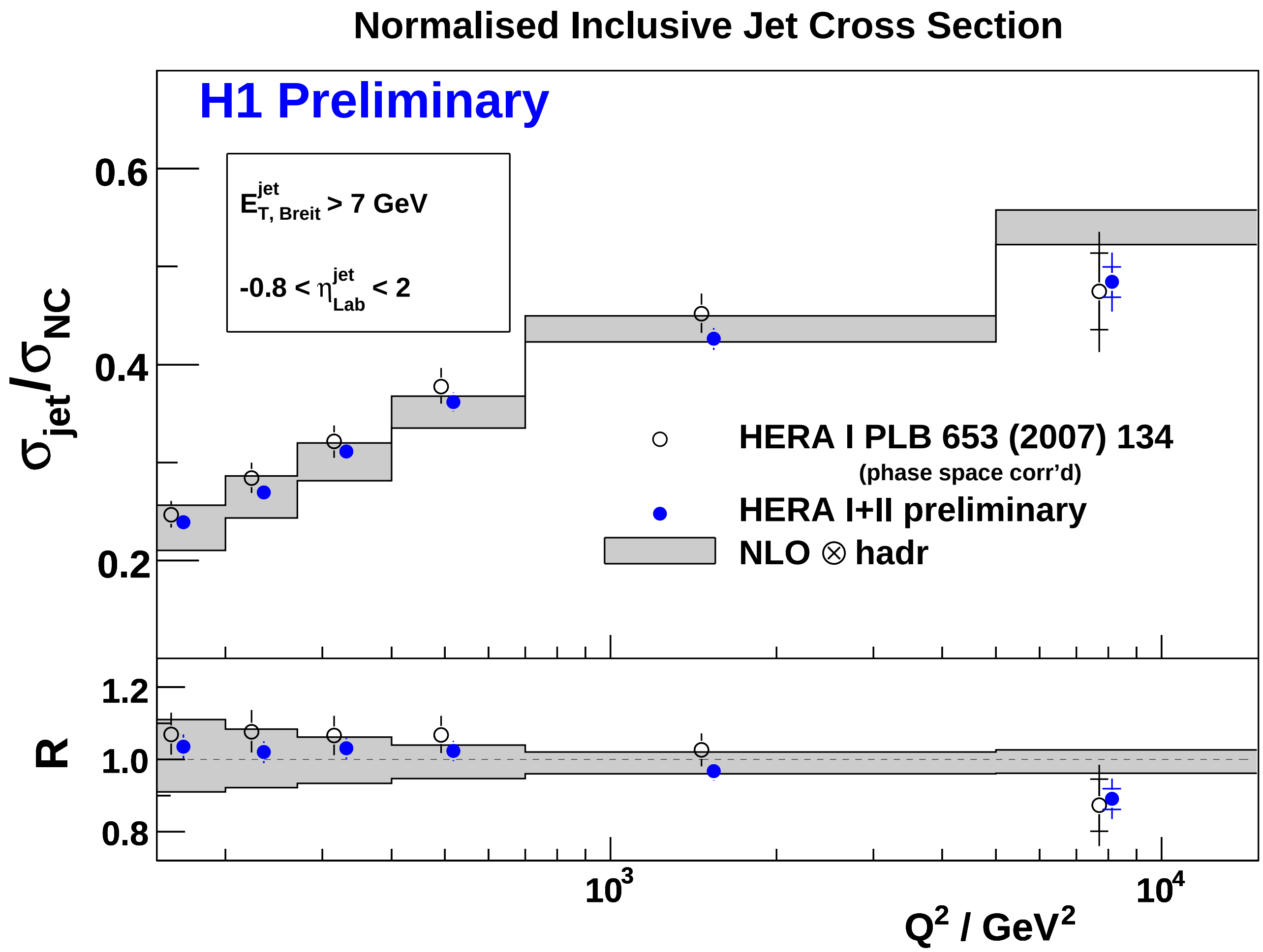

Figure 9: Cross section for inclusive jets in the Breit frame, with $E_T > 7$ GeV. The values are normalised to the total neutral current cross section at a given value of Q^2.

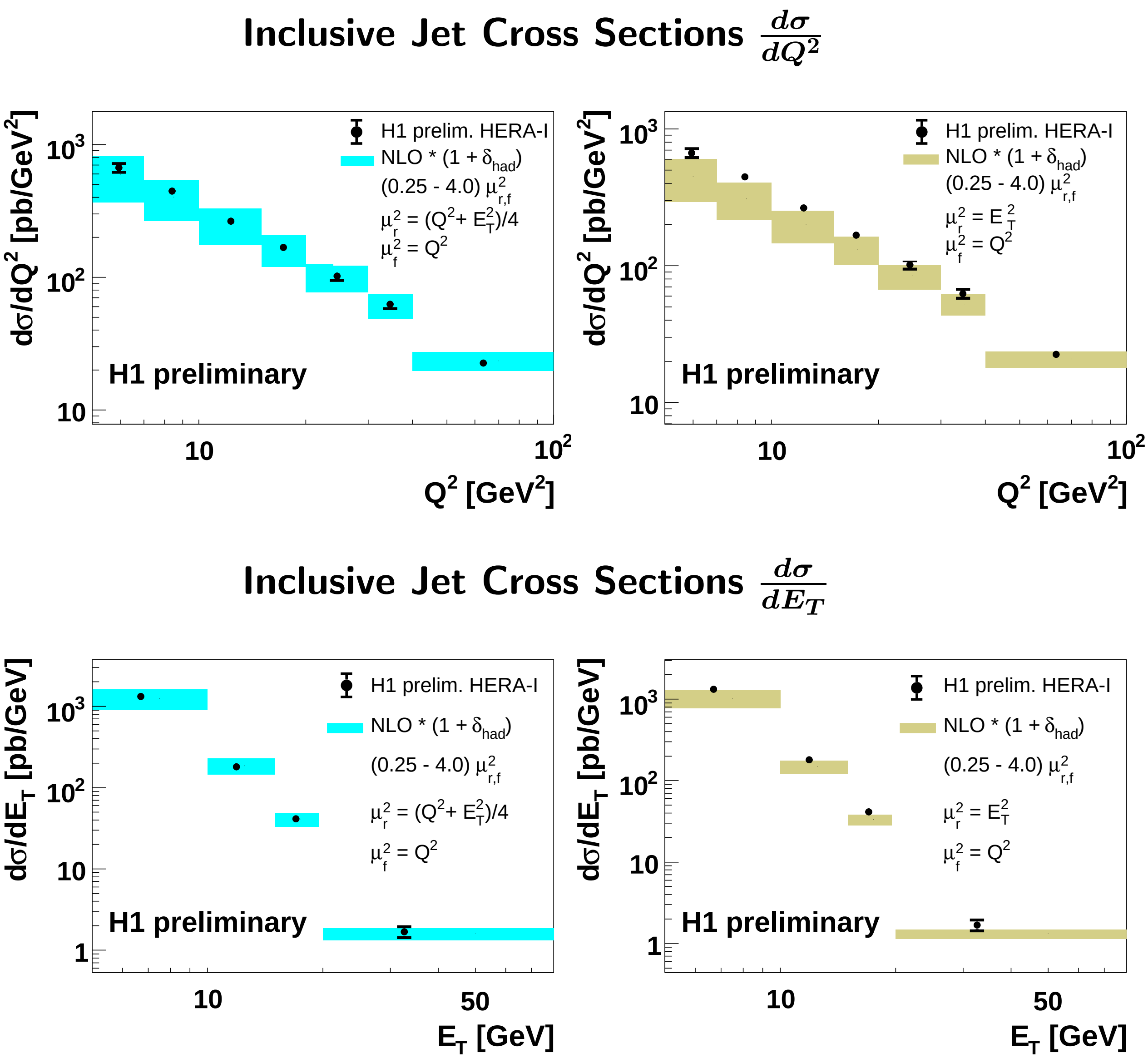

Figure 10: H1 differential cross section values for inclusive jets in the Breit frame in DIS for a lower range of Q^2 values. Left: standard renormalisation scale; right: variant renormalisation scale.

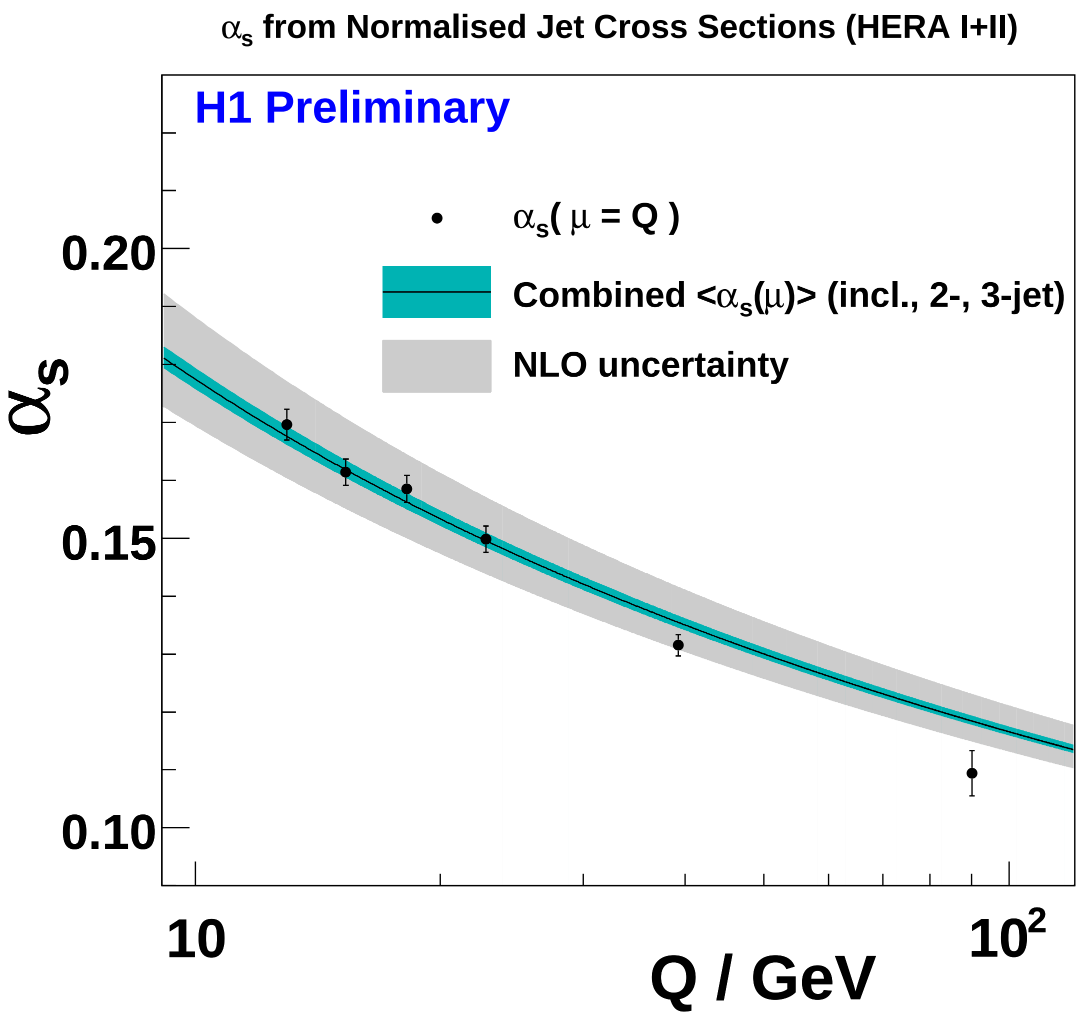

Figure 11: Fitted values of α_s from H1 data at high Q^2, as a function of Q. The narrow central band indicates experimental uncertainties and the broader outer band indicates theoretical uncertainties.

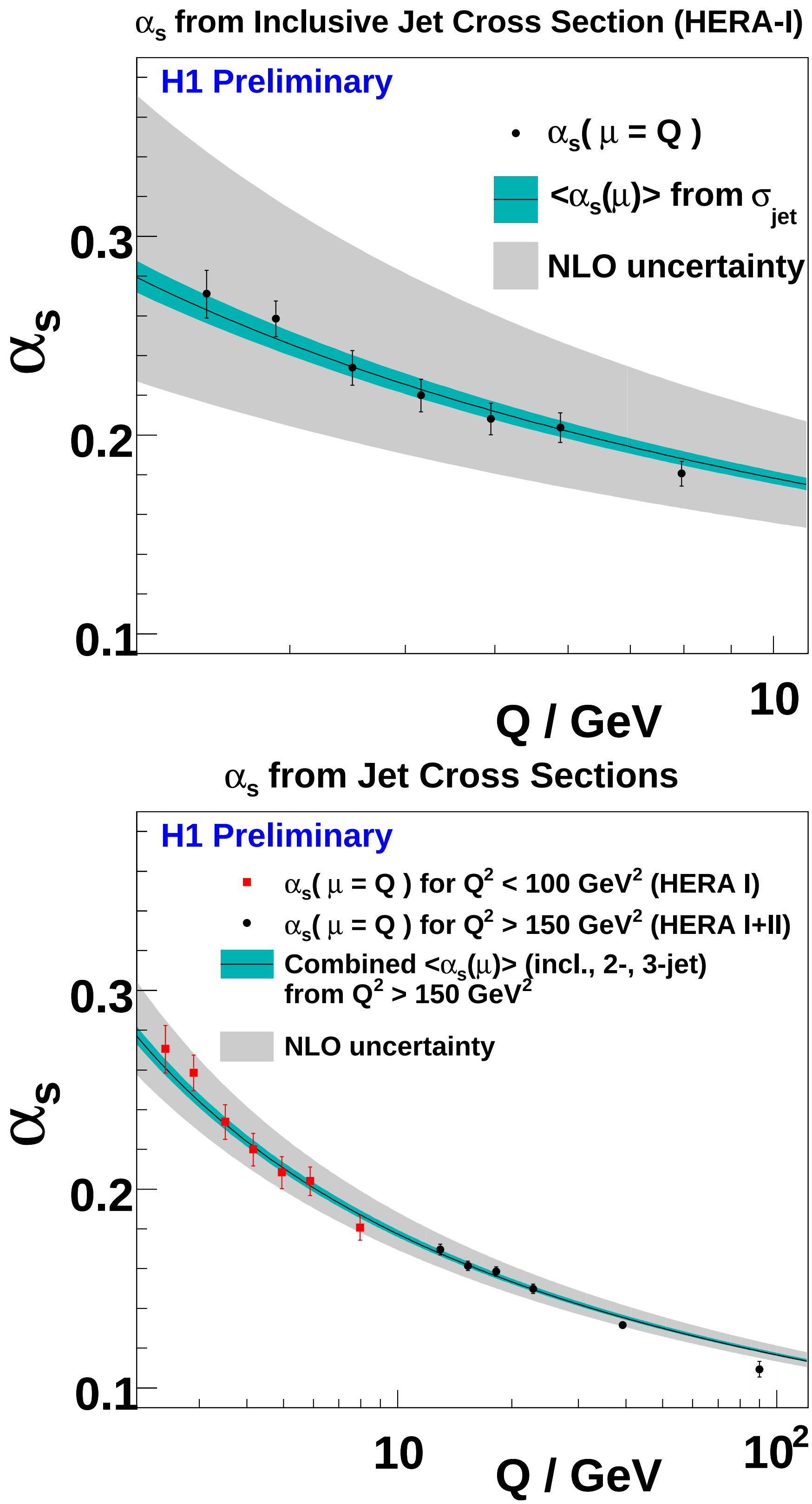

Figure 12: Fitted values of α_s from H1 data at high Q^2, as a function of Q. The narrow central band indicates experimental uncertainties and the broader outer band indicates theoretical uncertainties. In the lower plot the high-Q band is extrapolated into the low-Q region.

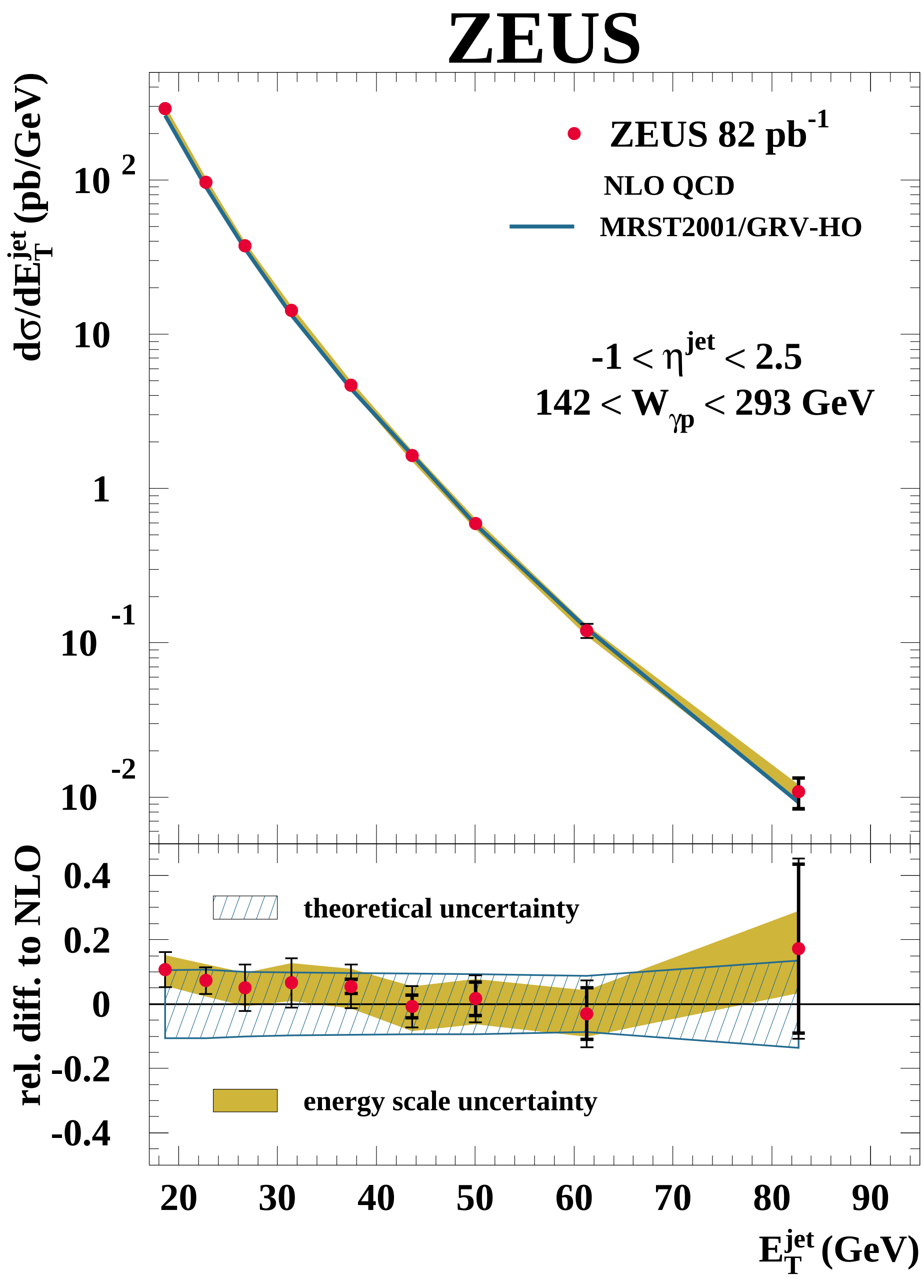

Figure 13: Inclusive jet distribution measured by ZEUS in photoproduction with $E_T > 17$ GeV, compared to NLO theory.

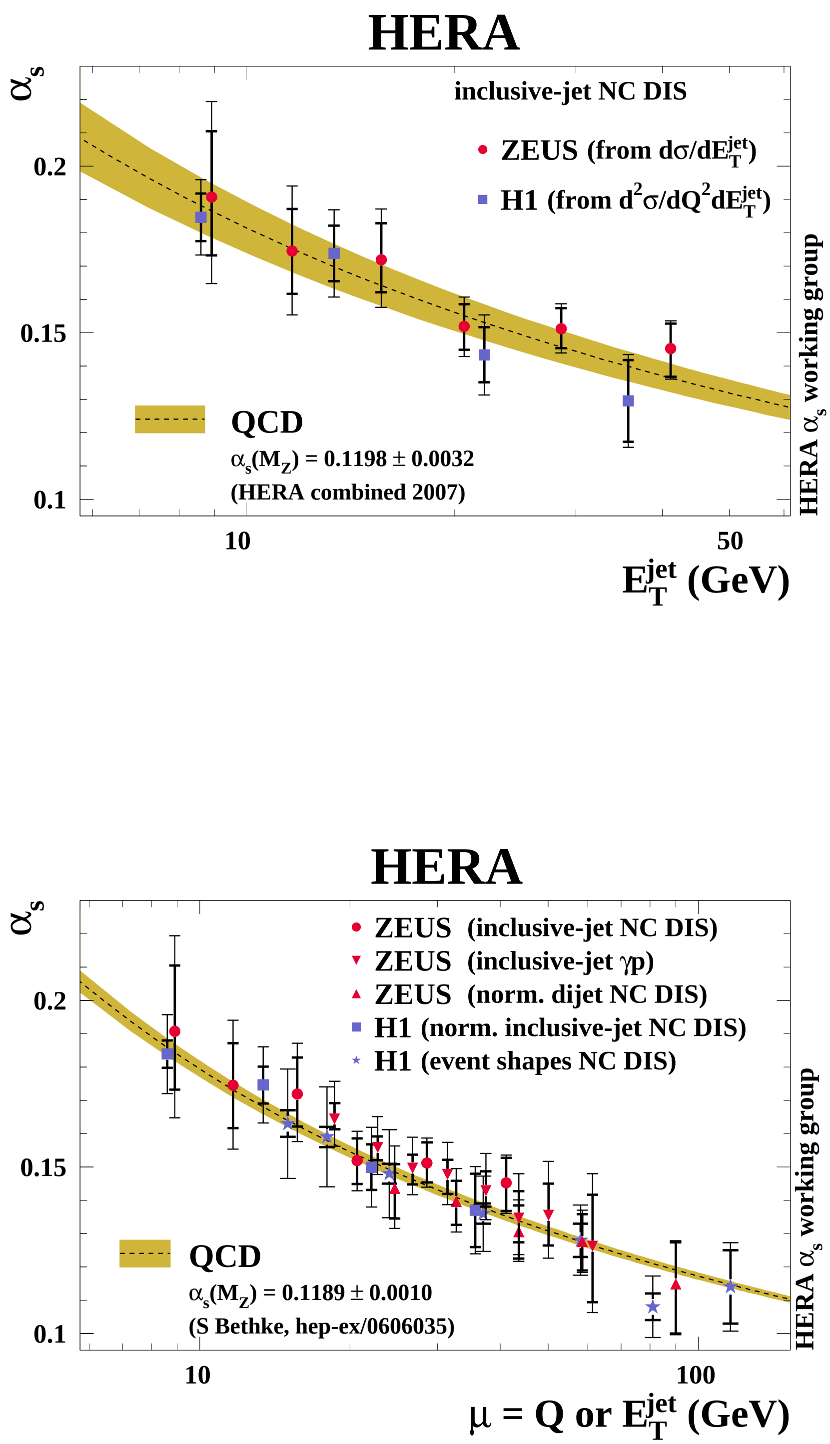

Figure 14: Fitted values of α_s from H1 and ZEUS data at high Q^2, as a function of Q. The top plot illustrates results from the combined fit; the lower plot includes a wider collection.

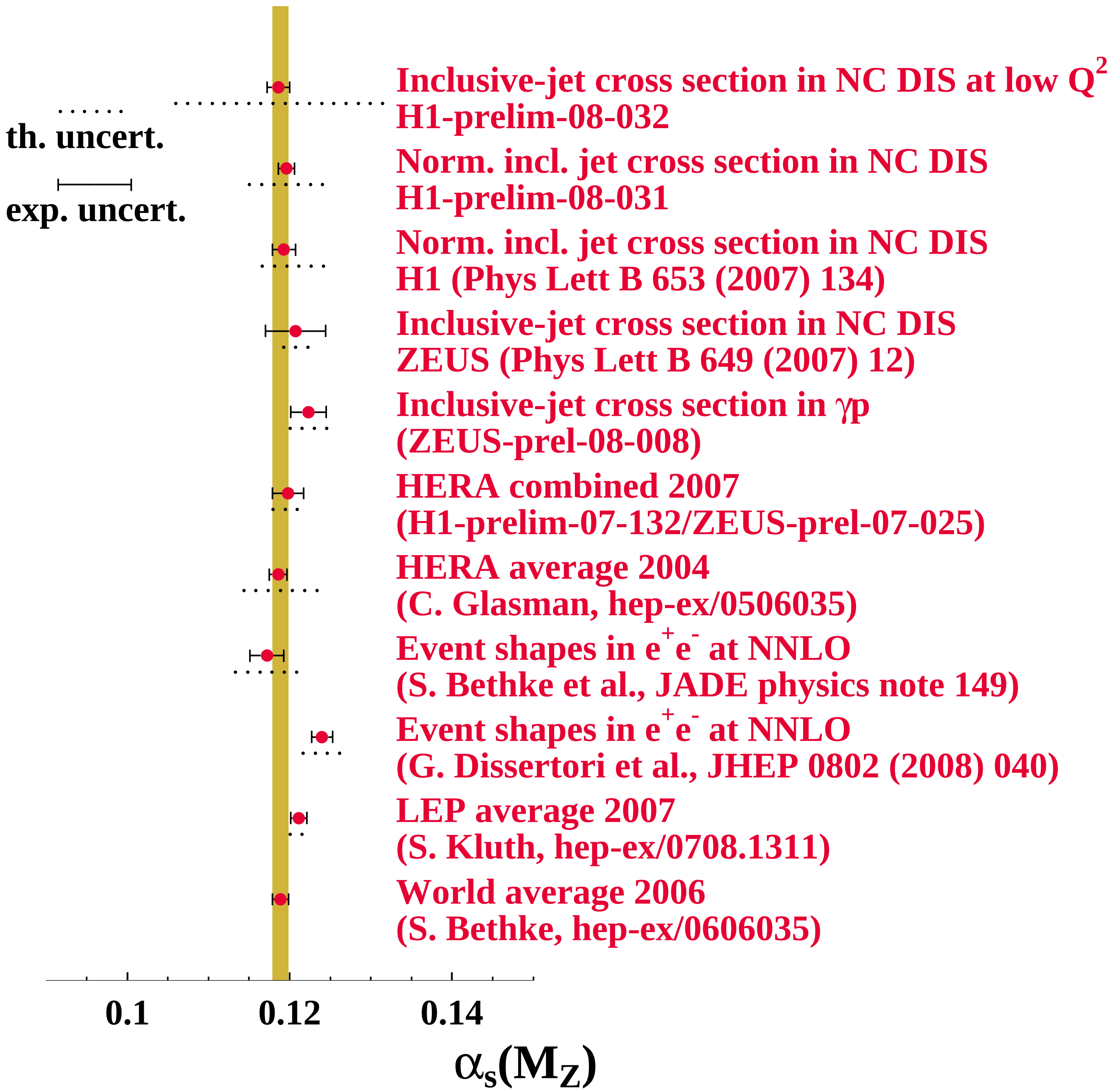

Figure 15: Comparison of various determinations of α_s with a world average value.